NASA Technical Memorandum 4598

X-29 Flight Control System: Lessons Learned

Robert Clarke, John J. Burken, John T. Bosworth,
and Jeffery E. Bauer

June 1994

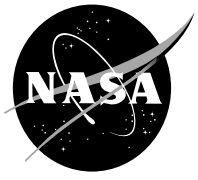

NASA Technical Memorandum 4598

X-29 Flight Control System: Lessons Learnedl

Robert Clarke, John J. Burken, John T. Bosworth,
and Jeffery E. Bauer
Dryden Flight Research Center
Edwards, California

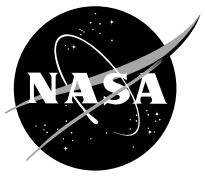

National Aeronautics and
Space Administration
Office of Management
Scientific and Technical
Information Program
1994

X-29 Flight Control System: Lessons Learned

Robert Clarke, **John J. Burken**, **John T. Bosworth**,
and Jeffrey E. Bauer
NASA Dryden Flight Research Center
Edwards, California 93523
United States of America

ABSTRACT
Two X-29A aircraft were flown at the NASA Dryden Flight Research Center over a period of eight years. The airplanes' unique features are the forward-swept wing, variable incidence close-coupled canard and highly relaxed longitudinal static stability (up to 35-percent negative static margin at subsonic conditions). This paper describes the primary flight control system and significant modifications made to this system, flight test techniques used during envelope expansion, and results for the low- and high-angle-of-attack programs. Throughout the paper, lessons learned will be discussed to illustrate the problems associated with the implementation of complex flight control systems.

1. NOMENCLATURE

ACC	automatic camber control (flight control system mode)
AOA	angle of attack
ARI	aileron-to-rudder interconnect
BMAX	rudder pedal command gain
$C_{L_{max}}$	maximum lift coefficient
CF	cost function
CP	constraint penalty
DP	design point
FCS	flight control system
FFT	fast Fourier transform
g	unit of acceleration, 32.2 ft/sec^2
G_{lim}	pitch stick limit gain
G_q	pitch rate feedback gain
$G_{\dot{q}}$	pitch acceleration feedback gain
G_{n_z}	normal acceleration feedback gain
GAIN1	pitch axis g-compensation gain
GH(s)	open-loop transfer function
GF1	symmetric flaperon gain factor
GS1	strake flap gain factor
GMAX	pitch stick command gain
GYCWSH	rudder pedal-to-aileron washout filter time constant
Hg	chemical symbol for the element mercury
HG(s)	loop gain matrix
I	identity matrix
ISA	integrated servoactuator
j	$\sqrt{-1}$
K2	roll rate-to-aileron feedback gain
K3	$\dot{\beta}$ -to-aileron feedback gain
K4	lateral acceleration-to-aileron feedback gain
K13	lateral stick-to-aileron forward-loop gain
K14	rudder pedal-to-aileron forward-loop gain
K17	$\dot{\beta}$ -to-rudder feedback gain
K18	lateral acceleration-to-rudder feedback gain
K27	lateral stick-to-rudder forward-loop gain
LOF	left outboard flaperon
LVOT	linear variable differential transducer
M	Mach number
MIMO	multi-input–multi-output
n_y	lateral acceleration, g
n_z	normal acceleration, g
NACA	National Advisory Committee for Aeronautics
p	roll rate, deg/sec
P_s	static pressure, inHg
PCE	pilot compensation error
PMAX	lateral stick command gain
q	pitch rate, deg/sec
Q_c	impact pressure, inHg
r	yaw rate, deg/sec
RDM	return difference matrix
RM	redundancy management
RPE	resonance peak error
s	Laplace transform variable

S_{aa}	generic auto spectrum of *a*
S_{ab}	generic cross spectrum of *a* to *b*
SF	scale factor
SISO	single-input–single-output
T_t	total temperature, °C
TE	trailing edge
V	true airspeed, knots
XKI1	pitch axis forward-loop integrator gain
XKI3	lateral axis forward-loop integrator gain
XKP1	pitch axis forward-loop proportional gain
XKP3	lateral axis forward-loop proportional gain
XKP4	yaw axis forward-loop proportional gain
XPITCH	pitch axis input sequence used in fast Fourier transform
YPITCH	pitch axis output sequence used in fast Fourier transform
α	angle of attack, deg
$\dot{\alpha}$	angle of attack rate, deg/sec
β	angle of sideslip, deg
$\dot{\beta}$	angle of sideslip rate, deg/sec
δ_a	differential flaperon deflection, deg
δ_{a_p}	lateral stick deflection, in.
δ_c	canard deflection, deg
δ_{e_p}	pitch stick deflection, in.
δ_f	symmetric flaperon deflection, deg
δ_r	rudder deflection, deg
δ_{r_p}	rudder pedal deflection, in.
δ_s	strake flap deflection, deg
θ	pitch angle, deg
σ_{SSV}	structured singular value
σ_{USV}	unscaled singular value
t	time constant
ϕ	bank angle, deg
ω	frequency, rad/sec

2. INTRODUCTION

The Grumman Aerospace Corporation (Bethpage, NY) designed and built two X-29A airplanes under a contract sponsored by the Defense Advanced Research Projects Agency (DARPA) and funded through the United States Air Force. These airplanes were built as technology demonstrators with a forward-swept wing, lightweight fighter design. The use of tailored composites allowed the forward-swept wing design to be fabricated without significant weight penalties.[1] Both airplanes were flown at the NASA Dryden Flight Research Center to test the predicted aerodynamic advantages of the unique forward-swept wing configuration and unprecedented level of static instability (as much as 35-percent negative static margin; time to double amplitudes were predicted to be as short as 120 msec). Early on, the airplane designers recognized many potential advantages of this configuration. The forward-swept wing results in lower transonic drag as well as better control at high angle of attack (AOA).[2] The configuration was designed to be departure resistant and maintain significant roll control at extreme AOA. The typical stall pattern of an aft-swept wing, from wingtip to root, is reversed for a forward-swept wing, which stalls from the root to the tip.

Through the eight years of flight test, over 420 research flights were flown by the two X-29A airplanes. These flights defined an envelope which extended to Mach 1.48, just over 50,000-ft altitude, and up to 50° AOA at 1 *g* and 35° AOA at airspeeds up to 300 knots.

The flight experience at low AOA (below 20° AOA) with the initial flight control system (FCS) is covered in less detail since this design was done by Grumman Aerospace Corporation.[3,4] Several flight test techniques will be addressed. These techniques include in-flight time history comparison with simple linear models and stability margin estimation (gain and phase margins) as well as new capabilities (structured singular value margins) which extend these single-loop stability measures to multiloop control systems. In addition, modifications to improve the FCS will be described, in particular a technique used to improve the handling qualities of the longitudinal axis will be discussed.

The design of the high AOA FCS modifications will be presented. Techniques used to expand the high-AOA envelope will be discussed as well as the problems discovered during this effort. An FCS design feature was the incorporation of a dial-a-gain that allowed two control system gains to be independently varied during flight. This feature allowed many control system changes to be evaluated efficiently. These experiments allowed rapid incorporation of flight derived improvements to the FCS performance.

3. TEST AIRPLANE DESCRIPTIONS

The X-29A research airplane integrated several technologies, e.g., a forward-swept, aeroelastically tailored composite wing and a close-coupled, all moving canard. Furthermore, the wing, with a 29.27° leading-edge sweep and thin, supercritical airfoil, is relatively simple employing full-span, double-hinged, trailing-edge flaperons which also provide discrete variable camber. All roll control is provided by these flaperons, as the configuration does not use spoilers, rolling tail, or differential canard. The airplane has three surfaces used for longitudinal control: all moving canards, symmetric wing flaperons, and aft-fuselage strake flaps. The lateral–directional axes are controlled by differential wing flaperons (ailerons) and a conventional rudder. The left and right canards are driven symmetrically and operate at a maximum rate of approximately 100°/sec through a range of 60° trailing-edge (TE) up and 30°

TE down. The wing flaperons move at a maximum rate of 68°/sec through a range of 10° TE up and 25° TE down. The rudder control surface has a range of ±30° and a maximum rate of 141°/sec. The strake flaps also act within a range of ±30°, but have a maximum rate of only 27°/sec.

The second X-29A (fig. 1) was modified for high-AOA testing by adding a spin parachute which was attached at the base of the vertical tail. The spin parachute was installed to provide for positive recovery from spins, as spin-tunnel tests had indicated that the X-29A ailerons and rudder provided poor recovery from fully developed upright spins. The addition of an inertial navigation system and the spin parachute system increased the empty weight of the airplane by almost 600 lb.

4. LOW-ANGLE-OF-ATTACK RESEARCH

Research at low AOA was the focus of all flight testing on X-29A No. 1 throughout its four years of flight test.[5–7] Initially, the focus (from a flight control designer's viewpoint) was on proving adequate stability margins and fixing problems which impacted stability or redundancy management. In the last year of flying, the focus was shifted to make improvements to the FCS to overcome the deficiencies which had been identified by the pilots. The X-29A No. 2 airplane was used primarily to examine high-AOA characteristics, but was also used to study the stability margins of the lateral–directional axes using multi-input–multi-output (MIMO) techniques at low-AOA conditions.

4.1 Description of the Flight Control System

The X-29A airplane is controlled through a triplex fly-by-wire FCS, which was designed for fail-operational, fail-safe capability. A schematic of the FCS is shown in fig. 2. Each of the three channels of the FCS incorporates a primary mode digital system using dual central processing units along with an analog reversion mode system. Both the digital and analog systems have dedicated feedback sensors. The digital computers run with an overall cycle time of 25 msec. The commands are sent to servoactuators that position the aerodynamic control surfaces of the airplane.

The initial longitudinal axis control laws were designed using an optimal model following technique.[4] A full-state feedback design was first used with a simplified aircraft and actuator model. The longitudinal system stability was significantly affected as higher order elements, such as sensor dynamics, zero-order-hold effects, actuators and time delays, were added to the analysis.[3] To recover the lost stability margins, a conventional design approach was taken to develop lead–lag filters to augment the basic control laws. Even after the redesign work, the stability margin design requirements were relaxed by the contractor to 4.5 dB and 30° (if all of the known high-order dynamics were included in the analysis). The government flight test team decided to require the use of flight measured stability margins and set minimum margins at 3 dB and 22.5°.

Figure 3 is a block diagram of the longitudinal control system. Short-period stabilization is achieved mainly through pitch rate and synthesized pitch acceleration feedback. Normal acceleration feedback is used to shape the stick force per *g*. The proportional-plus-integral compensation in the forward loop improves the short-period response and steady-state response to pilot inputs. Positive speed stability, which is important during powered approach, is provided by either automatic engagement or pilot selection of airspeed feedback.

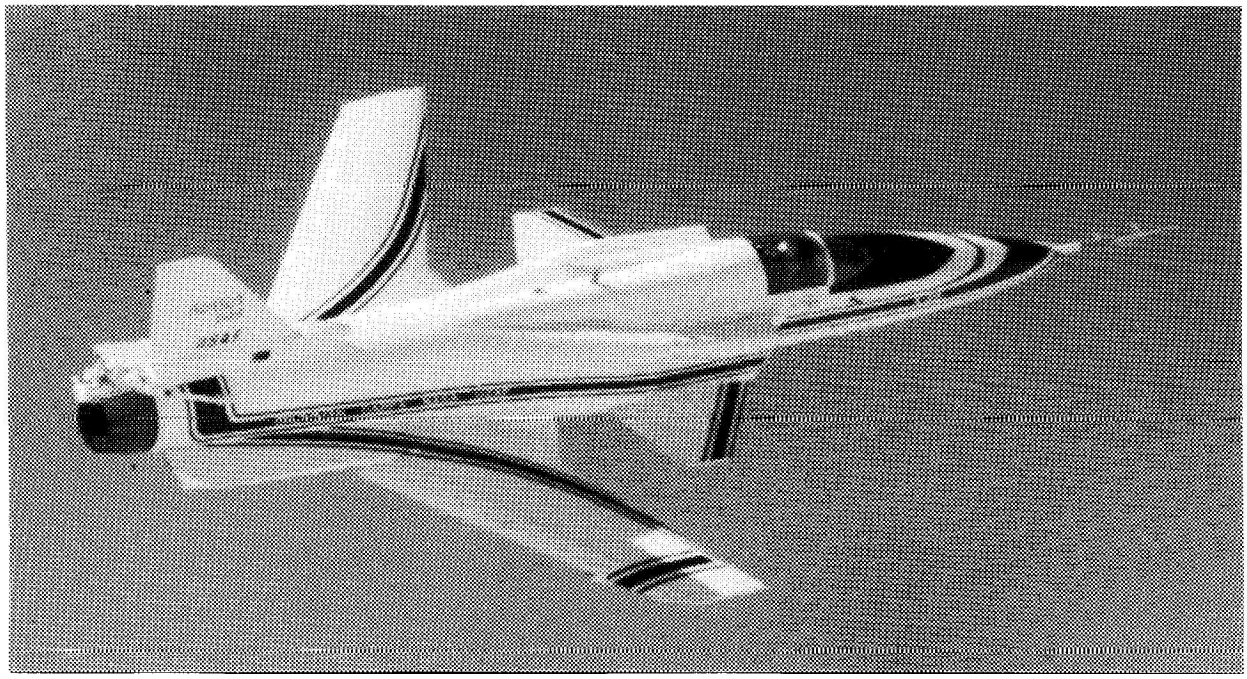

EC 89 0321-3

Figure 1. X-29A No. 2 airplane.

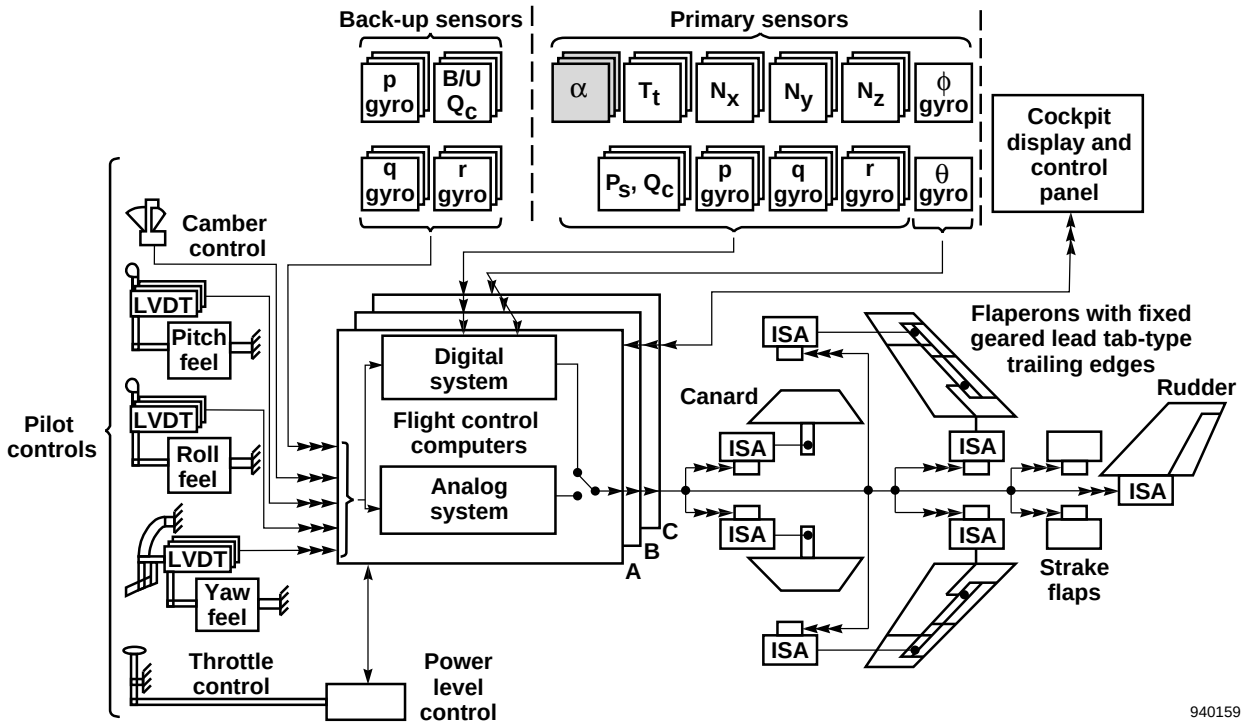

Figure 2. X-29A flight control system. (Note: Number of arrowheads designate level of redundancy and highlighted blocks represent changes made for high AOA.)

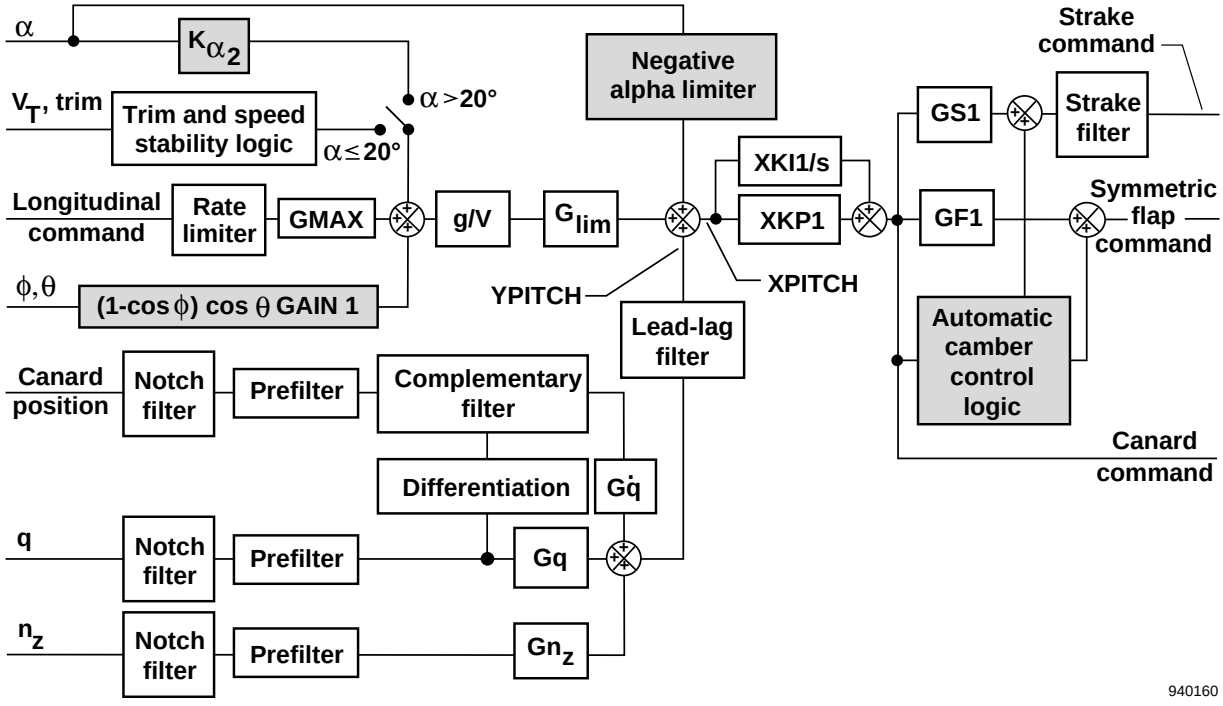

Figure 3. X-29A longitudinal control system. (Note: Highlighted blocks represent changes made for high AOA.)

In addition to the short-period stabilization function, the primary mode includes an automatic camber control (ACC) function which, in steady flight, generates commands to the symmetric flaperons and strake flaps to optimize the overall lift-to-drag ratio of the airplane. The dynamic characteristics of the ACC feedback loops were designed to be significantly slower than those of the basic stability augmentation loops.

Figure 4 is the lateral–directional control law block diagram. The bare airframe lateral–directional characteristics of the X-29A are stable, and the multivariable FCS is conventional.[3] Roll rate is proportional to the lateral stick deflection through a nonlinear gearing gain that enhances the precision of small commands while still enabling the pilot to command large roll rates with larger stick deflections. A command rate limiter is implemented in the roll and yaw axis control systems to minimize the potential of control surface rate limiting, caused by large commands. Another feature is the forward-loop integrator in the roll axis which provides for an automatic trim function and helps to null steady-state roll errors. Synthetic sideslip rate feedback is used to provide dutch roll damping and to assist in turn coordination. An aileron-to-rudder interconnect (ARI) is also used to help coordinate rolls commanded with lateral stick deflections alone.

4.2 Flight Test Techniques

The following section presents some of the tools used to analyze the X-29A aircraft. The three tools used for flight data analysis were single-input–single-output (SISO) stability margins, time history comparisons, and MIMO or multivariable robustness margins. The first two tools were applied in near real-time during envelope expansion of X-29A No. 1, while the last one was only used in postflight analysis on X-29A No. 2. Both stability margin analyses, SISO and MIMO, obtained the desired frequency responses without physically opening any of the feedback loops.

4.2.1 *Single-input–single-output gain and phase margins*

Aircraft that have a high degree of static instability, like the X-29A, require close monitoring in the early envelope expansion stages of flight test. Fast Fourier transformation (FFT) techniques were used to measure the longitudinal open-loop frequency response characteristics over the entire flight envelope.

The X-29A longitudinal control system architecture lends itself to classical SISO stability margin analysis. As shown in fig. 3, the feedback paths reduce to a single path, allowing for traditional gain and phase margin analysis, such as Bode analysis. To excite the vehicle dynamics, a series of pilot pitch stick commands or computer generated frequency sweeps were used. Briefly, the technique collects the time domain variables XPITCH and YPITCH driven by the sweep, and uses an FFT to estimate the open-loop transfer function *GH(s)*. The open-loop frequency response is displayed on a monitor, and gain and phase margins are determined. The details of the near real-time SISO frequency response technique can be found in reference 8.

The frequency response of a SISO system can be estimated from the auto and cross spectra of the input and output. An estimate of the open-loop response is defined as

$$GH(j\omega) = \frac{S_{xy}}{S_{xx}} = \frac{S_{yy}}{S_{xy}} \qquad (12.1)$$

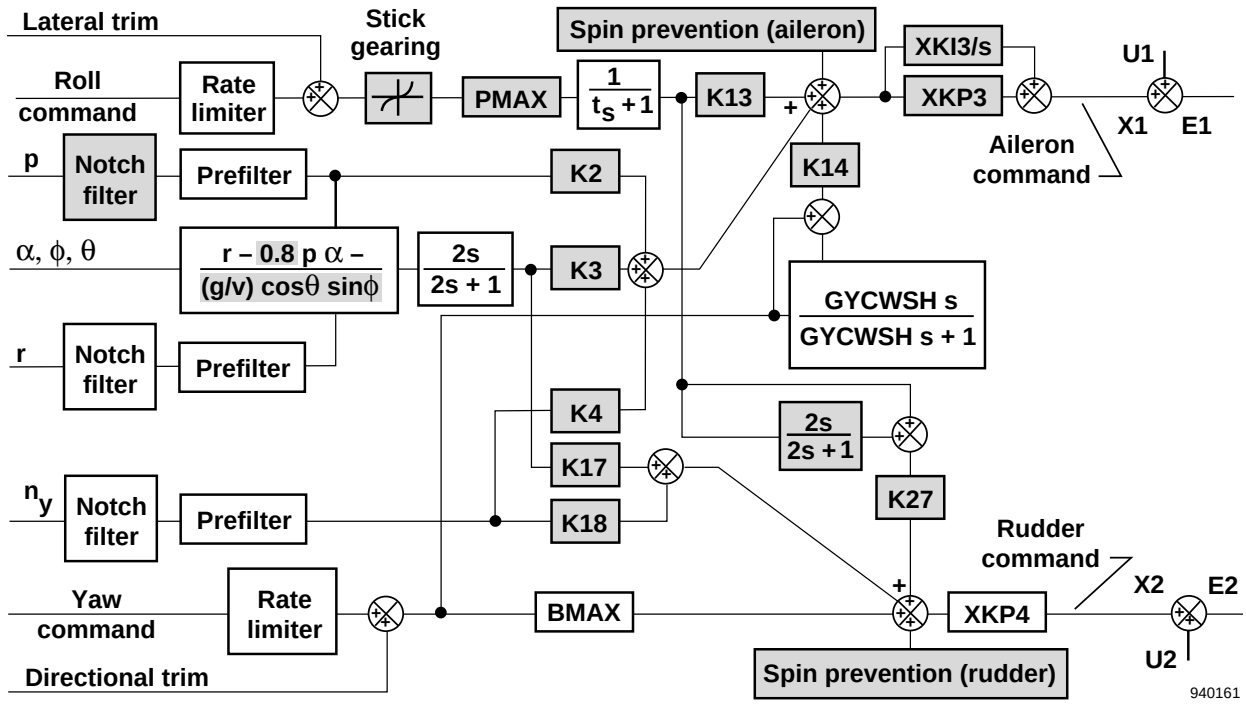

Figure 4. X-29A lateral–directional control system. (Note: Highlighted blocks represent changes made for high AOA.)

where S_{xy} is the cross spectrum of the input XPITCH with the output YPITCH, S_{xx} is the auto spectrum of the input, and S_{yy} is the auto spectrum of the output. The overall procedure is shown in fig. 5.

This test technique revealed much lower (below the established flight test minimum margins) than expected margins at a low-altitude transonic flight condition. As a result, the overall longitudinal loop gain was reduced to recover adequate stability margins. The actual amount of the reduction came directly from the comparison of predicted gain and phase margins with the analytical estimates. Once the control law change was made, the measured stability margins were greater than the requirement.

It was found that open-loop SISO frequency responses could be measured in-flight without physically breaking the loop. The near real-time capability enhanced the efficiency of the X-29A envelope expansion program. Gain margins greater than 3 dB and phase margins higher than 22.5° were eventually demonstrated over the entire flight envelope.

4.2.2 *Linear model time history comparisons*

The real-time comparison of the airplane response with linearized models allows the flight test personnel to verify the aircraft is performing as predicted, to determine regions of nonlinear behavior, and to increase the rate of envelope expansion.[9] Direct comparison of the measured aircraft response to those generated by a simulation, driven with identical pilot inputs, provides timely information. It is an extremely useful test tool if the comparison between the actual and simulation response can be made in real time.

Regions of nonlinear behavior of the aircraft can easily be determined. For example, surface rate limits show up dramatically when the flight data are compared to the linear simulation response. Knowledge of this nonlinear behavior can be useful in interpreting differences among results from other data analysis procedures, such as frequency response methods or parameter estimation techniques.

The success of the time history comparisons depends on a detailed and accurate math model. For the X-29A airplane the models were obtained by linearizing the nonlinear equations of motion about a trimmed flight condition. The perturbation step sizes were ±1 percent of Mach number for total velocity, ±2° for angle of attack, and ±1° or deg/sec for the remaining states and control surfaces. These step sizes provided reasonable estimates of the linear coefficients.

4.2.3 *Multi-input–multi-output stability margins*

The X-29A lateral–directional control system is a MIMO system, and the classical frequency analysis methods are inadequate for this type of control system. The classical methods, such as Bode or Nyquist analysis, do not allow for simultaneous variations of phase and gain in all of the feedback paths.[10–12] Recently, singular value norms of the return difference matrix (RDM = $I + GH(s)$ or $I + HG(s)$) have been considered a measure of the system stability margins for multivariable systems.[10,11,13] However, singular value norms of a system can be overly conservative, and a control system designer could

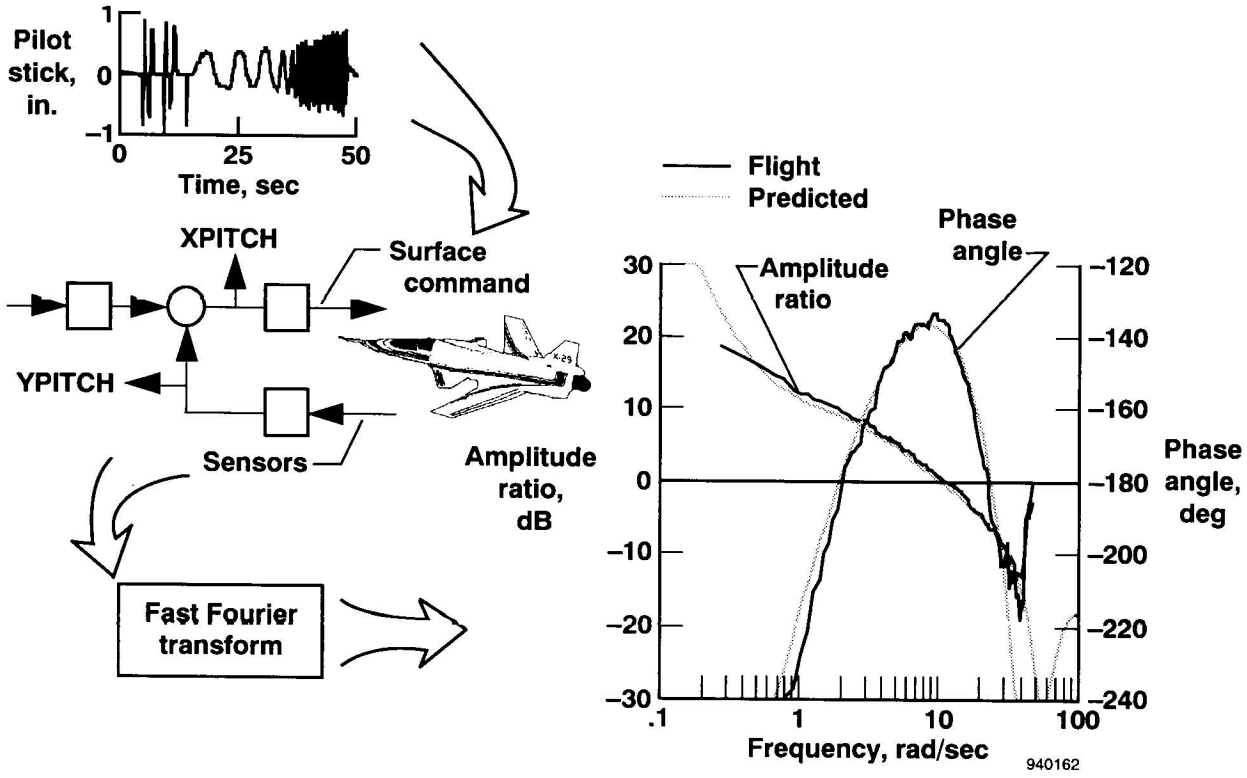

Figure 5. Near real-time determination of longitudinal axis open-loop frequency response from flight data.

interpret the results as unsatisfactory when, in fact, the system is robust.[12] A method for relieving the excessive conservatism is derived by structuring the uncertainties.[10,11]

To evaluate the stability robustness of a multivariable system, the Dryden Flight Research Center conducted a series of flight test maneuvers on the X-29A No 2.[14] The flight singular value technique was compared with predicted unscaled singular values (σ_{USV}), structured singular values (σ_{SSV}), and with the conventional single-loop stability margins. Although flight singular values were determined postflight, this analysis can be used for near real-time monitoring and safety testing.

As the minimum singular value ($\underline{\sigma}$) of the input or output RDM approaches zero, the system becomes increasingly less stable. The flight singular values need to be determined by using frequency response techniques. A complex frequency response of a system can be estimated from the auto spectrum and cross spectrum of the input and output time history variables by transforming these time domain responses to the frequency domain using the FFT. The controller input-to-output transfer matrix, $\mathbf{X}_u(s)$ is defined as follows

$$\mathbf{X}_u(s)_{ij} = \sum_{k=1}^{N} (S_{x_j u_i}(s))_k (S_{u_i u_i}(s))_k^{-1} \qquad (12.2)$$

where $S_{xu}(s)$ is the cross spectrum of the input u and output x, $S_{uu}(s)$ is the auto spectrum of the input, and N is the number of time history arrays.

Using the relationship defined in eq. (12.2), the open-loop gain matrix is

$$\mathbf{HG}(s) = \mathbf{X}_u(s)(\mathbf{I}-\mathbf{X}_u(s))^{-1} \qquad (12.3)$$

Figure 6 shows the flight-determined minimum singular values, $\sigma[\mathbf{I} + \mathbf{HG}(s)]$, as well as analytical scaled structured and unscaled structured singular values. This plot shows that good agreement exists between the flight and analytical data. The analytical σ_{SSV} tend to agree slightly better with the flight data than with the analytical σ_{USV}.

For comparison purposes, the classical single-loop frequency response results (SISO) are shown in the following table along with the singular value (MIMO) analysis. These MIMO margins were obtained using the universal phase and gain relationship.[15] The MIMO analysis allows for simultaneous independent variations, while the SISO analysis allows for single-loop variation.

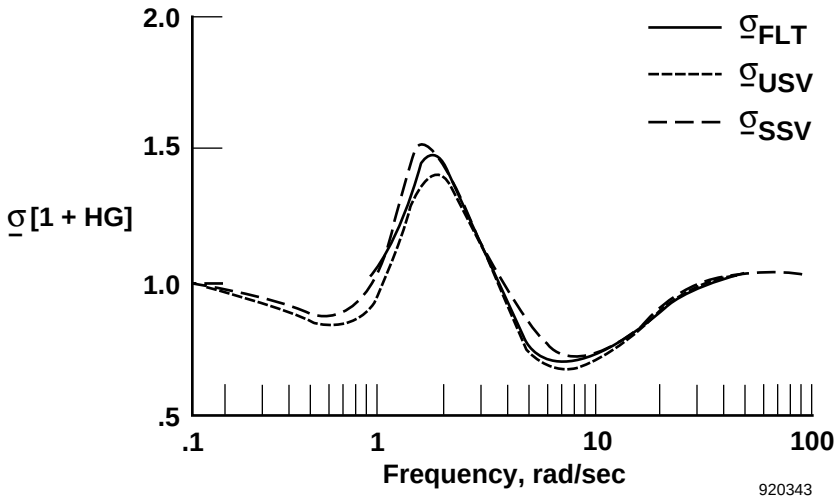

Figure 6. Flight and predicted minimum singular values of X-29A at Mach 0.7, 30,000-ft altitude, with baseline gain set.

Comparison of SISO and MIMO lateral–directional stability margins at Mach 0.7 and 30,000-ft altitude.

	Multiple-input–multiple-output			Single-input–single-output	
	σ_{USV}	σ_{SSV}	σ_{FLT}	Lateral	Directional
$\underline{\sigma}$	0.65	0.72	0.72		
Gain margin, dB	8.5	11.5	11.5	18	13
frequency, rad/sec	8	8	8	17	13
Phase margin, deg	35	41	41	77	62
frequency, rad/sec	8	8	8	2.5	4.5

The minimum stability margin determined by the SISO method is 13 dB and 62°; whereas the flight singular value (MIMO) method resulted in a margin of 11.5 dB and 41°. As expected, the singular value method is conservative, but the results between the SISO and MIMO methods are similar. This is not surprising at this low-AOA condition since the X-29A lateral axis is largely uncoupled from the directional axis.

Extracting multiloop singular values from flight data and comparing the information with prediction validates the use of flight singular values as a relative measure of robustness. This comparison increases the confidence in using structured singular values for stability assessments of multiloop control systems. In addition, this technique extends the single-loop gain and phase margin concepts to multiloop systems.

4.3 Control Law Modifications

Several changes in the flight control system were required as a result of the high level of instability of the X-29A. A significant change was made to the air data selection logic. The initial control laws used three equally weighted sources (a single noseboom and two side probes) for total pressure measurements. The most accurate source, the noseboom measurement, was almost never used by the flight control system since it was usually an extreme, not the middle value. To compensate, a change was made to use the noseboom as long as it was within the failure tolerance of the middle value. This change came back to haunt the test team as the failure tolerance was very large and it was discovered that a within-tolerance failure could result in such large changes in feedback gains that the longitudinal control system was no longer stable.

The flight data showed that reducing the tolerance to an acceptable level (going from 5.0 to 0.5 inHg) would not work as there was a narrow band in AOA from 7° to 12° where errors on the side probe measurements were as large as –1.5 inHg (airplane really faster than indicated). This large error was caused by strong forebody vortices which enveloped one or both of the air data probes located on the sides of the fuselage. The solution was a 2.0-inHg tolerance and a bias of 1.5 inHg added to the side probe measurements. This worked since the sensitivity to the high gain condition (airplane faster than indicated) was much greater than that of the low gain condition (airplane slower than indicated). The airplane had been operated for almost three years before this problem was identified and fixed.

The high level of static instability of the X-29A caused the control law designers to stress robustness over handing qualities. During flight test the aircraft models were refined, which allowed the control system to be fine tuned to improve the handling qualities.[6] To keep it simple, there was a strong desire to fine tune the control system without drastic changes in the system architecture. The process used to provide improved handing qualities involved four steps: selection of design goals, selection of design variables, translation of the design goals into a cost function, and iterative reduction of the cost function.

The Neal–Smith analysis provided a good quantitative method for assessing predictions of handling qualities. Unlike lower order equivalent system analysis, the Neal–Smith technique applies to systems that do not exhibit classical second-order behavior. In addition, there is no ambiguity introduced by the goodness of fit of the higher order system to a low-order match. The Neal–Smith method takes the longitudinal stick position to pitch rate (or attitude) transfer function, and closes the loop around it with a simple compensator, representative of a simple pilot's transfer function. The compensator consists of a lead–lag filter with a gain and a time delay (fig. 7). The application of the Neal–Smith criterion to the X-29A baseline control laws indicated a relatively large amount of lead required of the compensator to obtain the desired tracking performance. This correlated well with the pilot's comments which indicated a desire for increased pitch responsiveness in tracking tasks.

The design goals were to obtain quicker pitch response without adversely affecting the stability, control surface activity, or introducing a pilot induced oscillation problem. The point defined as the desired Neal–Smith criterion was nominally 0 dB and 10° (fig. 8). A real scalar cost function (CF) was defined as follows

$$CF = RPE + PCE/SF + CP \qquad (12.4)$$

where the resonant peak error (RPE) is the distance between the achieved resonant peak and desired peak (0 dB). The pilot compensation error (PCE) is the distance between the achieved pilot compensation and the desired compensation (10°). The constraint penalty (CP) is 10,000 if either the stability margin or surface activity constraints were violated, and 0 otherwise. The scale factor (SF) is 7.0, which is commonly used to compensate for the difference in magnitude of the units of decibels and degrees.

Reference 6 covers the background and details of the improved handling qualities optimization of the X-29A airplane. The design goal of 10° of lead and 0 dB resonant peak was not achieved because of the design constraints; however, the amount of pilot lead was reduced by approximately 50 percent. The closed-loop resonant peak achieved by the modified gains was below 1.0 dB. This resulted in Neal–Smith criterion which

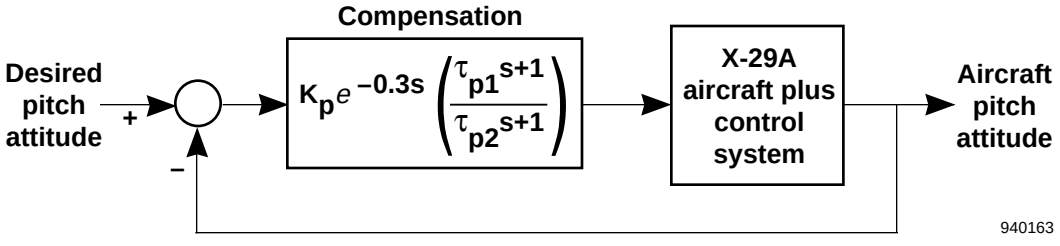

Figure 7. Closed-loop pitch attitude tracking task.

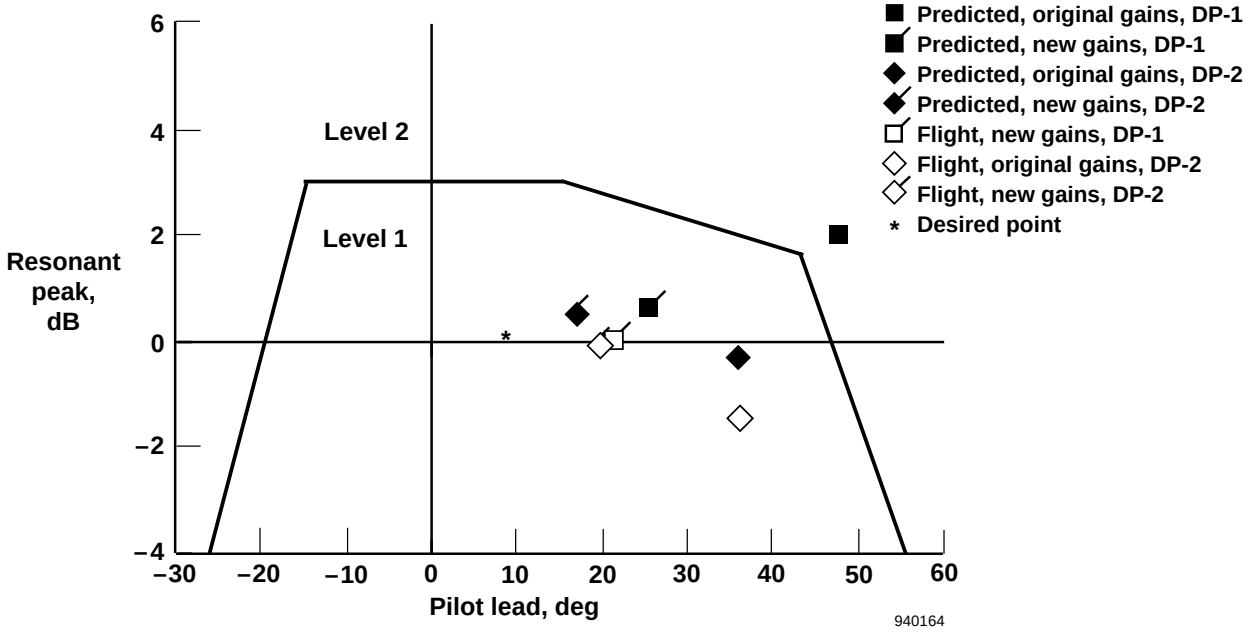

Figure 8. Neal–Smith analysis comparing the modified gains with the original gains for predicted and flight test results. (NOTE: DP represents design point.)

was well within the level 1 region of the Neal–Smith plane. The design process showed a definite trade-off between the constraints and the achievable Neal–Smith criterion. The modified design gains showed a slightly reduced level of stability margin and increased surface activity. In general, the pilot comments indicated a marked improvement in the performance of the new FCS software.

This design methodology provided a practical means for improving the handling qualities of the vehicle without excessive system redesign. The method provided a 100-percent increase in the pitch acceleration (from 16°/sec^2 to 32°/sec^2) with precise control. The final design for the X-29A exhibited a problem associated with rate limiting which resulted in a lower phase margin than predicted. Fortunately the rate limiting problem occurred at frequencies higher than the range used by a pilot in handling qualities tasks.

5. HIGH-ANGLE-OF-ATTACK RESEARCH

Research at high AOA was the focus of all flight testing on X-29A No. 2. The control laws were modified for high AOA and several airplane modifications were made to assure that the program could be conducted safely. The flight tests were conducted to discover the AOA limits of maneuvering flight (which had been predicted to be up to 40° AOA) and symmetric pitch pointing flight (which was predicted to be as great as 70° AOA). The initial control laws were designed conservatively with provisions made for improvements if the flight data indicated that additional performance would not compromise stability.

5.1 Description of the Flight Control System

The control laws were designed to allow “feet-on-the-floor” maneuvering with the lateral stick commanding stability axis roll rate and the longitudinal stick commanding a blended combination of pitch rate, normal acceleration, and AOA. Rudder pedals commanded washed out stability axis yaw rate which allowed the airplane to be rolled using the strong dihedral of the airplane at up to 40° AOA.

This approach for controlling a blend of pitch rate and AOA at high AOA is different from the design philosophy of the F-18 High Alpha Research Vehicle and X-31 Enhanced Fighter Maneuverability airplanes which are primarily AOA command systems. The blended combination of feedbacks used in the X-29A FCS provided more of an $\dot{\alpha}$-type command system with weak AOA feedback. The pitch axis trim schedule provided small positive stick forces at 1-*g* high-AOA conditions (approximately 1-in. deflection or 8-lb force required to hold 40° AOA).

The high-AOA FCS was designed using conventional techniques combined with the X-29A nonlinear batch and real-time simulations. Linear analysis was used to examine stability margins and generate time histories which were compared with the nonlinear simulation results to validate the results. The linear analysis included conventional Bode stability margins, time history responses, and limited structured singular value analysis in the lateral–directional axes. In the pitch axis stability margins at high-AOA conditions were predicted to be higher than the stability margins at the equivalent low-AOA conditions. However, in the lateral–directional axes the unstable wing rock above 35° AOA dominated the response in linear and nonlinear analysis. Feedback gains which could stabilize the linear airplane models showed an unstable response in the nonlinear simulation driven by rate saturation of the ailerons. The control system design kept the feedback gains at a reason-

able level and allowed the low-frequency unstable lateral–directional response.

5.1.1 *Design goals*

The FCS design was required to retain the low-AOA flight characteristics and control law structure which had been previously flown on X-29A No. 1. It was further required that the control system ensure that spins would not be easily entered, which required an active spin prevention system.

In the lateral axes the airplane was controlled with conventional ailerons and rudder. The ailerons had priority over symmetric flaperon deflections in the control laws. The control laws were designed in this manner since all roll control was provided by the ailerons and pitch control was provided by canards, strake flaps, and symmetric flaperons.

5.1.2 *Design of the longitudinal axis*

For the most part, the basic low-AOA X-29A normal digital longitudinal axis control laws remained unchanged at high AOA. No gains in the longitudinal axis were scheduled with AOA, but several feedback paths were switched in and out as a function of AOA. The following changes (which are highlighted in fig. 3) were made in the design of the high-AOA control laws for the X-29A longitudinal axis:

1. Modified ACC schedules which were designed to provide optimum lift-to-drag ratio canard and strake positioning at high AOA. This provides increased maximum attainable lift and reduced transonic canard loads.

2. Fade-out of velocity feedback and fade-in of AOA feedback to control a slow divergent instability. Velocity feedback was not appropriate to control the instability which developed at high AOA; AOA provided the best feedback as the divergence was almost purely AOA.

3. Active negative AOA- and *g*-limiters designed to prevent nose-down pitch tumble entries and potential inverted hung stall problems.

4. Fade-out of single-string attitude–heading reference system feedbacks. The attitude information only provided gravity compensation for pilot inputs and n_z feedback. The single-string nature and relatively small benefit did not warrant the risk of system failure at high AOA conditions.

5. Symmetric flaperon limit reduction from 25° to 21°. Because high-gain roll rate feedback would be required to prevent wing rock and because the wing flaperons are shared symmetrically and asymmetrically, 4° of flaperon deflection were reserved for aileron type commands. The flaperons are commanded with differential commands having priority. At high AOA the ACC schedule would otherwise command the wing flaperons on the symmetric limit and result in a coupling of the wing rock and longitudinal control loop through the symmetric flaperon.

During the accelerated entry high-AOA envelope expansion, the aft stick authority limit was reached earlier than expected (at 25° AOA full aft stick was reached for 160 and 200 knots). The original high-AOA FCS was limited, as were all previous X-29A FCS releases, to 5.4 incremental *g* command at high speed and 1.0 incremental *g* at low speed. The FCS modification increased this to 7.0 (+30 percent) incremental *g* command at high speed and 2.0 (+100 percent) *g* at low speed.

A functional check flight of the FCS change showed that although the stick sensitivity was changed it was still acceptable (since stick feel characteristics were unchanged, any change in command authority changes stick force per *g*). The X-29A pilots noted that during 1-*g* flight at 35° and 40° AOA "... the increased sensitivity of the longitudinal control was evident, but compensation by the pilot was easily accomplished."

5.1.3 *Design of the roll–yaw axes*

In the lateral–directional axes the control laws were changed significantly at high AOA from the original low-AOA control system. The lateral–directional block diagram (fig. 4) shows a full-state type feedback structure. The high-AOA changes, for the most part, were simplifications in the control law structure flown on X-29A No. 1. The new control laws required many gains to be scheduled with AOA; several were just faded to constants while four command and feedback gains used three AOA breakpoints for table lookup. These three AOA breakpoints were the maximum allowed because of computer space limitations. Computer speed limitations required that a multirate gain lookup structure be incorporated since AOA (20 Hz) was expected to change more rapidly than Mach number or altitude (2.5 Hz). The control law changes and reasons for them include the following:

1. The forward-loop integrator in the lateral axis was removed at high AOA. This eliminated a problem with the integrator saturating and causing a pro-spin flaperon command.

2. Most lateral–directional feedbacks were eliminated. This left only high-gain roll rate feedback-to-aileron and washed-out stability axis yaw rate feedback-to-rudder. The high-gain roll damper was used to suppress the wing rock which developed near $C_{L_{max}}$. The washed-out stability axis yaw rate or $\dot{\beta}$ feedback helped control sideslip during airplane maneuvers at high-AOA conditions.

3. Pilot forward-loop gains were also simplified, leaving only lateral stick-to-aileron, lateral stick-to-rudder, and rudder pedal-to-rudder. The lateral stick gearing was changed from second-order nonlinear gearing to linear gearing at high AOA and a wash-out filter was used in parallel with the ARI gain to provide an extra initial kick on rudder command.

4. Spin prevention logic was added which commanded up to full rudder and aileron deflection if yaw rate exceeded 30°/sec with AOA ≥40° for upright spins and AOA ≤–25° for inverted spins. The pilot command gain was increased to allow the pilot sufficient authority to override any of these automatic inputs.

At high AOA, vertical fin buffeting was encountered because of forebody vortex interaction. The control system was strongly affected through the excitation of several structural modes which were seen on the roll rate gyro signal. The buffet intensity was as high as 110 *g* at the tip of the vertical fin.

The vertical fin excited the roll rate gyro and through high-gain feedback, caused the flaperon actuators to attempt to track this high-frequency signal. Flight tests showed an unexpected hydraulic system problem resulted from this flaperon command. During a 360°-full stick aileron roll, the left outboard flaperon (LOF) hydraulic logic indicator showed a failure of the control logic for this actuator. The most probable explanation was that a flow restriction existed in the hydraulic lines driving the LOF and that this restriction showed up when large, high-frequency demands were placed on the actuator. Postflight analysis also showed that the measured LOF rates were approximately 7° to 8°/sec lower than for the right outboard flaperon.

Since the roll rate gyro signal did not originally use any structural notch filters, the vertical fin first bending (15.8 Hz), wing bending antisymmetric (13.2 Hz), and fuselage lateral bending (11.1 Hz) structural modes showed up in the commands to the ailerons. Figure 9 shows the response of the roll rate gyro. The figure shows that most of the vertical tail buffet is transferred to the roll rate gyro through the vertical fin first bending mode. Analysis of the flight data showed that the *g* level increased proportionately with dynamic pressure.

Notch filters and a software gain reduction on roll rate feedback were used as the long-term FCS solution to the problem. Before these changes, fifty percent of the maneuvers in the region of failures indicated LOF hydraulic logic failures. After the changes were made, these failure conditions occurred only rarely and even more severe entry conditions and higher buffet levels were encountered without incident.

5.1.4 *Other changes*

To aid in research and to allow for unknown problems in flight testing, several additional changes were made to the control system. These changes included a dial-a-gain capability to allow the roll rate-to-aileron and the ARI gains to be independently varied (K2/K27). These two gains can each have five different values.

Concerns about the severe wing rock had led to a slow build-up in AOA using the dial-a-gain variations. The airplane roll response was found to be heavily damped and the dial-a-gain system was used to examine reductions in feedback gain. The response of the airplane was significantly quicker (approximately 20 percent) with the reduced roll rate feedback-to-aileron gain. No objectionable wing rock developed because of the lower gain.

Wing rock was predicted to be a major problem with the X-29A configuration at high AOA. These predictions had been made based upon wind-tunnel[16,17] estimates and supported by drop model flight tests.[18] Early simulation predictions were that wing rock would effectively limit the useful high-AOA envelope to approximately 35° AOA. Wing rock was predicted to deteriorate quickly as the roll damping became unstable and the limited aileron control power was insufficient to stop it. Roll rate-to-aileron gains as high as 2.0 deg/deg/sec were required to damp wing rock and prevent roll departures on the NASA Langley Research Center X-29A drop model. Flight tests with the dial-a-gain system showed that the K2 (roll rate-to-aileron) gain could be reduced from the initial maximum value of 0.6 to 0.48 deg/deg/sec with no significant wing rock. Decreases of this gain were required to assure that a rate limit driven instability in the ailerons at high dynamic pressures would not occur.

The second use of dial-a-gain was to increase the roll performance of the X-29A at high-AOA conditions. The stability axis roll rates were almost doubled in the AOA region from 20° to 30° at 200 knots (from 40°/sec to 70°/sec) with only small degradation in the roll coordination. Above this AOA, uncommanded reversals were seen because of control surface saturation and corresponding lack of coordination (predominantly increased sideslip). This performance improvement was accomplished with a 75-percent increase in the K13 (lateral stick-to-aileron) gain and an 80-percent increase in the K27 (lateral stick-to-rudder) gain. Increases in rates were possible

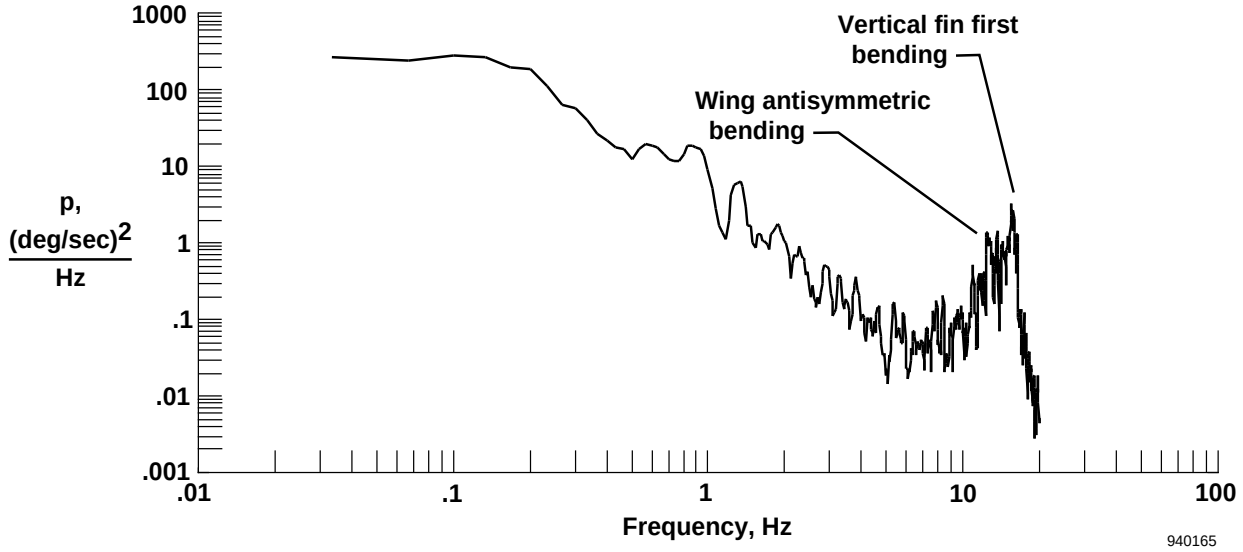

Figure 9. Roll rate gyro power spectral density.

throughout much of the high AOA envelope, but usually not as dramatic as this example. The dial-a-gain concept proved a valuable research tool used to test simple control law changes before the full FCS changes were made.

5.1.5 *Air data system*

Air data issues were addressed early in the development of the high AOA control laws. Measurement of accurate AOA was very important as this would be a primary gain scheduling parameter as well as a feedback to longitudinal and lateral–directional axes. Accurate air data were also important because of conditional stability of the lateral and longitudinal axes at high AOA. Stability margins would be compromised if air data errors were large.

Two of the three AOA sensors, located on each side of the airplane, had a range limited to 35°. The location and range were considered inadequate and two options were considered to solve the problem. The first option, to mount two additional AOA vanes on the noseboom, was mechanized and flown on X-29A No. 1 for evaluation and found to have excellent characteristics. The second option was to install NACA booms and AOA vanes on the wingtips. This option would have resulted in additional problems as the FCS did not rate correct its AOA measurements. With large lateral offsets, roll rate corrections would have to have been included which would have made AOA measurements sensitive to airspeed measurement errors. In the end, simplicity drove the decision to install two additional AOA vanes on the noseboom.

The second issue concerned accurate measurement of airspeed at high-AOA conditions caused by local flow effects. Several unsuccessful alternate pitot probe locations were investigated. Belly probes were tested on a wind-tunnel model and were found to change the aerodynamics, while swivel probes proved unable to be flight qualified for installation forward of engine inlets on a single-engine airplane. Since an alternate location could not be found, and the side probes were expected to have poor high-AOA characteristics, the decision was made to use a single string noseboom pitot-static probe at high AOA.

The high-AOA control system design had to be highly reliable. In general, multiple (three or more) sensors were used to provide redundancy, but for impact pressure at high AOA the FCS relied on a single noseboom probe with two independent sensors.

The air data system was carefully monitored during the high-AOA expansion. Differences between the noseboom and side probes were tracked as a function of AOA and compared with redundancy management trip levels (which were 1.5 inHg for static pressure, 2.0 inHg for total pressure, and 5.0° for AOA). Predictions about the air data system made during the FCS design were found to be pessimistic because the system worked better than expected. With the exception of the known problem with the total pressure measurements in the 7°- to 12°-AOA region, the maximum error at all other conditions was less than 0.5 inHg. In hindsight the flight data showed that the side probes performed adequately for FCS gain scheduling purposes and the system did not need to be made single string on the noseboom probe.

One in-flight incident occurred because of the air data system. Figure 10 shows the time history of a recovery maneuver. The figure shows that as sideslip exceeded 20°, the left rear AOA vane exceeded the sensor tolerance and was declared failed. This incident occurred during a recovery from 50° AOA. The airplane continued to operate on the two remaining sensors and

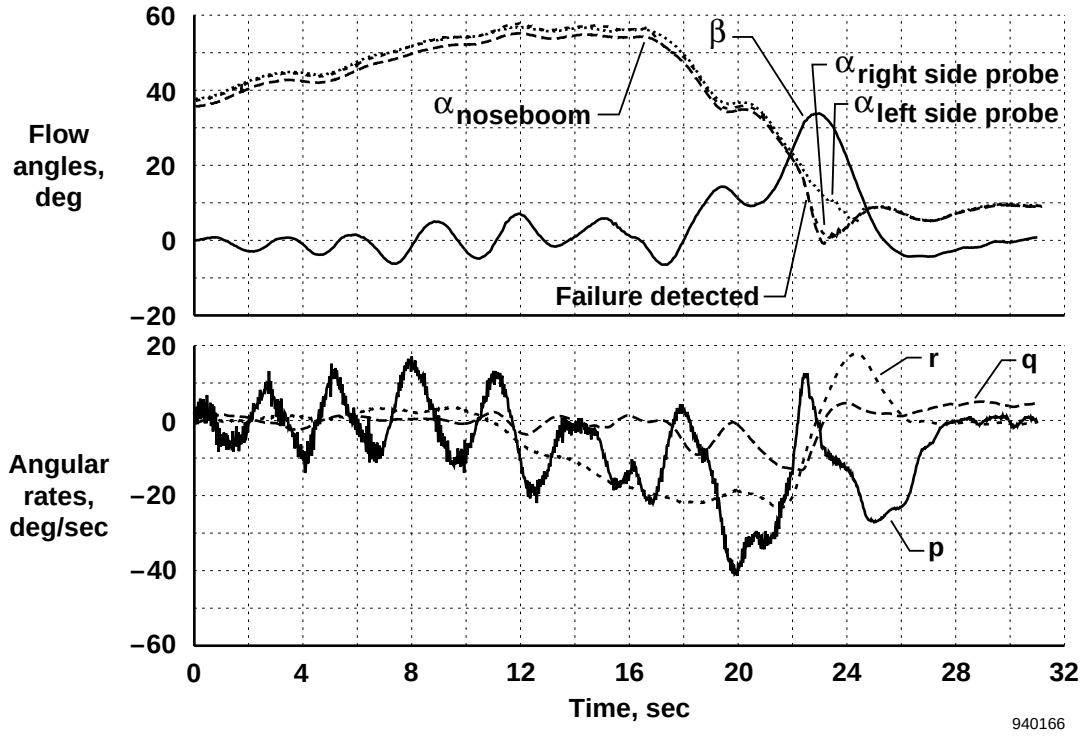

Figure 10. Angle-of-attack redundancy management failure from flight 27—time histories.

was in no danger. Once the failure was known, the personnel in the control room were able to examine the individual AOA channels and discover that all vanes appeared to be functioning properly.

5.2 Envelope Expansion Technique

To increase the rate of envelope expansion, an incremental simulation validation technique[19] from the F-14 high-AOA ARI test program was refined and used. This analysis technique was used for postflight comparisons and model updating. It allowed the simulation aerodynamic model to be updated between flight days with local improvements, e.g., changes to lateral control power, derived from previous test points. This allowed the pilots to train with a simulation which matched the most important aerodynamic characteristics and provided engineers with a method to track the aerodynamic differences which were discovered in flight test. The magnitudes and types of changes to the aerodynamic model provided assurance that the airplane could be safely flown to the next higher AOA test point.

The updated aerodynamics were applied primarily in the lateral–directional axes as almost no changes were required in the longitudinal axis. The updates were constructed with mostly linear terms, but some local nonlinearities were also included.

The most important characteristics to match were the magnitude, frequency, and phase relationships of the airplane response. At first, attempts were made to use all six degrees-of-freedom in the simulation, but longitudinal trim differences caused the simulation to diverge from the flight measurements before the maneuver was complete. Since the lateral–directional dynamics were of primary importance, the longitudinal dynamics were separated from them. The simulation matching technique then used the measured longitudinal parameters and lateral–directional pilot stick and rudder pedal measurements as inputs to the batch simulation. This forced the airspeed, altitude, canard deflection, and AOA to track the flight measurements while allowing the lateral–directional axes complete freedom. Some work was also accomplished using an alternate technique which bypassed the control system and used the measured aileron and rudder as inputs, but the wing rock instability eventually made this too difficult. Without including the control system in the simulation the system is an unstable process, since the flight control system stabilizes the wing rock.

Several techniques were used to determine the aerodynamic model updates which would be made to the simulation model.[20] These updates were maintained in a separate aerodynamic delta math model which allowed quick and easy modification. Once the aerodynamic models were updated, sensitivity studies on the real-time simulation were used to predict the airplane response at the next flight test expansion points.

5.3 Pitch Rate Limitations

An example comparison of a full-stick pitch axis maneuver with the complete six degree-of-freedom baseline simulation is shown in figure 11. The flight maneuver required the pilot to trim the airplane in level flight at 10° AOA at 20,000-ft altitude (approximately 0.3 Mach). The simulation was matched to the

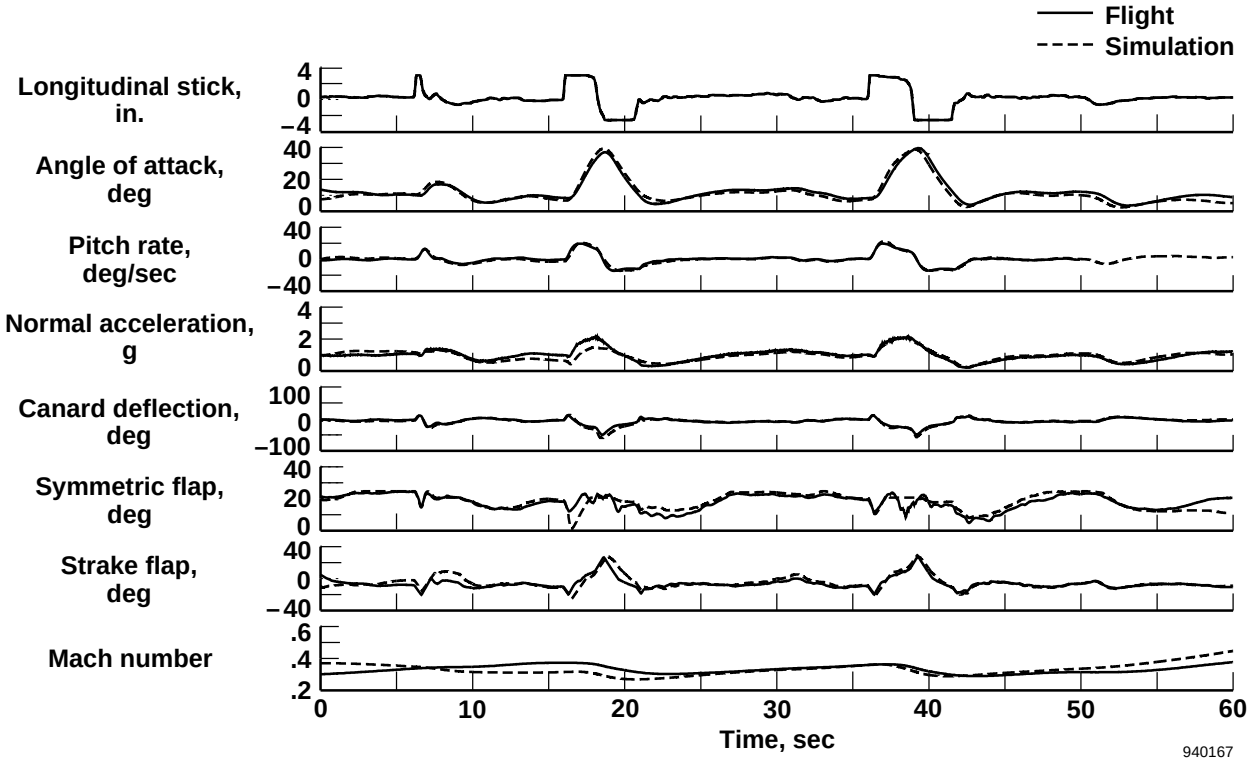

Figure 11. X-29 No. 2 flight/simulation comparison for large amplitude stick maneuver. Flight control software was the final high-AOA software.

initial trim condition and then driven with the pilot stick and throttle inputs. The figure shows close agreement between the flight data and simulation which allows a high confidence to be placed on simulation analysis of the X-29 pitch rate capability.

The X-29 pilots consistently found the maximum pitch rate capability of the airplane inadequate. Figure 12 shows the predicted maximum nose up and nose down pitch rates of the X-29 as a function of Mach number (altitude varied from 10,000 to 20,000 ft). Several flight data points (both nose up and nose down) from the maneuver shown in figure 11 are also included as well as F-18 pitch rate data for comparison purposes. The simulation maneuvers consisted of two types of maneuvers: a full aft stick step input and a doublet type input which consisted of a full aft stick input followed by a full forward stick input timed to try to force the control surfaces to maximum rates.

It is clear from the data that the X-29 requires approximately 50 percent higher rates to be comparable with an F-18 at low-speed conditions. Examination of the peak canard actuator rates shows that the X-29 was using nearly all of the capability (104°/sec no load rate limit) with the current control system gains. Increases in the canard actuator rates commensurate with the increases in pitch rate would be required for any improvement.

The simulation showed that most of the actuator rate was used in controlling the unstable airplane response. Figure 11 shows this in detail. Close examination of the canard response shows that during the full aft stick input the initial response of the canard is trailing edge down (and trailing edge up for the flaperon and strake flap). As is typical for an unstable pitch response the surfaces then move quickly in the opposite direction to unload and control the unstable response. The second motion is typically much larger than the initial motion and in most cases is more demanding of the actuator rates especially at low dynamic pressure where large control surface motion is required. This agrees very well with data presented in reference 4.

6. CONCLUSIONS

The X-29A airplanes were evaluated over the full design envelope. The flight control system successfully performed the tasks of stabilizing the short-period mode and providing automatic camber control to minimize trim drag. Compared with other highly augmented, digital fly-by-wire airplanes, the X-29A and its flight control system proved remarkably trouble free. Despite the unusually large, negative static margin, the X-29A proved safe to operate within the design envelope. Flight test showed the following lessons:

- Adequate stability to successfully test a 35-percent statically unstable airframe was demonstrated over the entire envelope in a *flight test research environment*. Extrapolations to a production–operational environment should be made carefully.
- The level of static instability and control surface rate limits did impact the nose up and nose down maximum pitch rates. At low airspeeds, to achieve rates comparable with an F-18, new actuators with at least 50-percent higher rate are required.
- Testability of a flight control system on an airplane with this level of instability is important and big payoffs can be made if provisions are made for real-time capabilities.

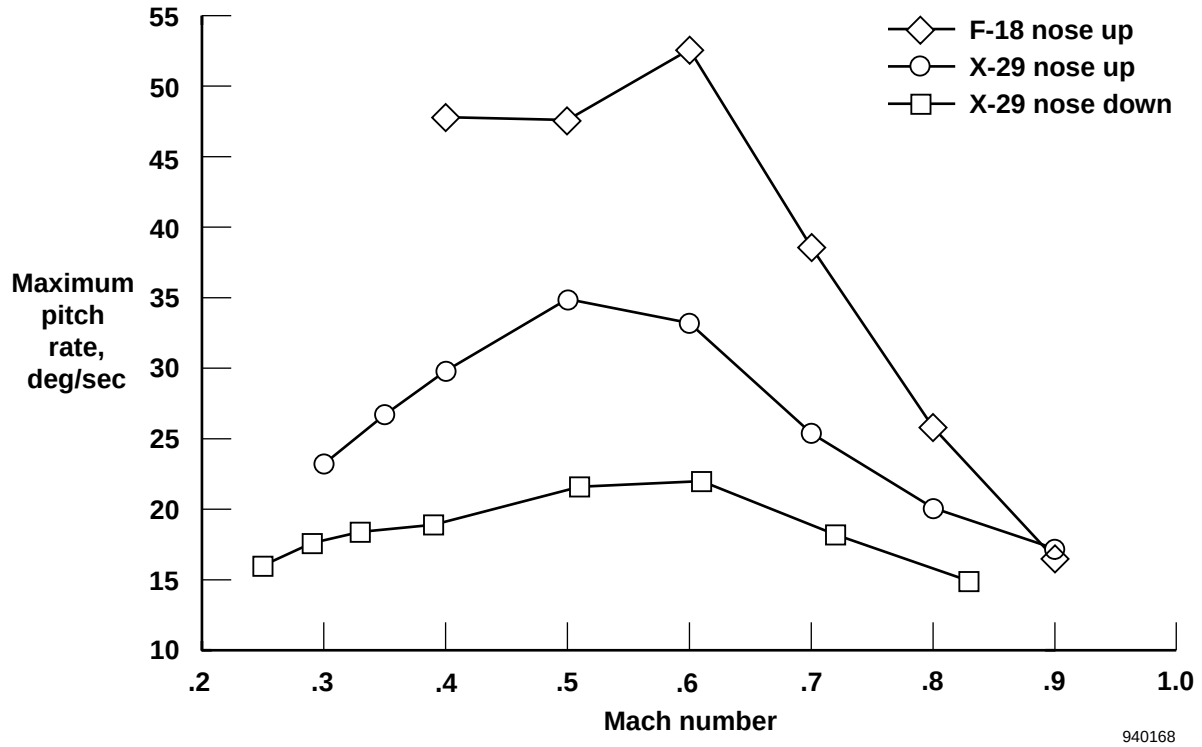

Figure 12. X-29 nose up and nose down pitch rate capability using final high-AOA flight control software.

- Air data are critical for highly unstable airframes and extra analysis is required to ensure adequate stability. Typical fighter type airplane air data redundancy management tolerances do not apply. Tight tolerances must be used even at the risk of nuisance failure detection.
- The dial-a-gain concept proved a valuable aid to evaluate subtle predicted differences in flying qualities through back-to-back tests. It was also useful to flight test proposed gain adjustments before major flight control system gain changes were made. This concept might not be easily applied to full state feedback designs, but forward-loop gains are good candidates for this use in any design.
- High angle of attack with high feedback gains will create problems with structural modes and require notch filters to eliminate flight control system response.

7. REFERENCES

1. Krone, N.J., Jr., "Forward Swept Wing Flight Demonstrator," AIAA Paper No. 80-1882, Aug. 1980.
2. Spacht, G., "The Forward Swept Wing: A Unique Design Challenge," AIAA Paper No. 80-1885, Aug. 1980.
3. Whitaker, A. and Chin, J., "X-29 Digital Flight Control System Design," AGARD CP-384: *Active Control Systems—Review, Evaluation and Projections*, Oct. 1984.
4. Chin, J., H. Berman, and J. Ellinwood, "X-29A Flight Control System Design Experiences," AIAA Paper No. 82-1538, Aug. 1982.
5. Gera, J., J.T. Bosworth, and T.H. Cox, *X-29A Flight Test Techniques and Results: Flight Controls*, NASA TP-3121, 1991.
6. Bosworth, John T. and Timothy H. Cox, *A Design Procedure for the Handling Qualities Optimization of the X-29A Aircraft*, NASA TM-4142, 1989.
7. Chacon, Vince and David McBride, *Operational Viewpoint of the X-29A Digital Flight Control System*, NASA TM-100434, 1988.
8. Bosworth, John T., *Flight-Determined Longitudinal Stability Characteristics of the X-29A Airplane Using Frequency Response Techniques*, NASA TM-4122, 1989.
9. Bauer, Jeffrey E., David B. Crawford, and Domenick Andrisani, "Real-Time Comparison of X-29A Flight Data and Simulations Data," AIAA Paper No. 87-0344, Jan. 1987; see also *J. Aircraft*, vol. 26, no. 2, Feb. 1989, pp. 117–123.
10. Doyle, John C. and Gunter Stein, "Multivariable Feedback Design: Concepts for a Classical/Modern Synthesis," *IEEE Transactions on Automatic Control*, vol. AC-26, no. 1, Feb. 1981, pp. 4–16.
11. Ly, Uy-Loi, "Robustness Analysis of a Multiloop Flight Control System," AIAA Paper No. 83-2189, Aug. 1983.
12. Paduano, James D. and David R. Downing, *Application of a Sensitivity Analysis Technique to High-Order Digital Flight Control Systems*, NASA CR-179429, 1987.
13. Newsom J.R. and V. Mukhopadhyay, "A Multiloop Robust Controller Design Study Using Singular Value Gradients," *J. Guidance, Control, and Dynamics*, vol. 8, no. 4, July–Aug. 1985, pp. 514–519.
14. Burken, John J., *Flight-Determined Stability Analysis of Multiple-Input–Multiple-Output Control Systems*, NASA TM-4416, 1992.
15. Mukhopadhyay, V. and J.R. Newsom, "A Multiloop System Stability Margin Study Using Matrix Singular Values," *J. Guidance, Control and Dynamics*, vol. 7, no. 5, Sept.–Oct. 1984, pp. 582–587.
16. Croom, Mark A., Raymond D. Whipple, Daniel G. Murri, Sue B. Grafton, and David J. Fratello, "High-Alpha Flight Dynamics Research On The X-29 Configuration Using Dynamic Model Test Techniques," SAE Paper No. 881420, Oct. 1988.
17. Murri, Daniel G., Luat T. Nguyen, and Sue B. Grafton, *Wind-Tunnel Free-Flight Investigation of a Model of a Forward-Swept-Wing Fighter Configuration*, NASA TP-2230, 1984.
18. Fratello, David J., Mark A. Croom, Luat T. Nguyen, and Christopher S. Domack, "Use of the Updated NASA Langley Radio-Controlled Drop-Model Technique for High-Alpha Studies of the X-29A Configuration," AIAA Paper No. 87-2559, Aug. 1987.
19. Gera, J., R.J. Wilson, E.K. Enevoldson, and L.T. Nguyen, "Flight Test Experience With High-α Control System Techniques on the F-14 Airplane," AIAA Paper No. 81-2505, Nov. 1981.
20. Pellicano, Paul, Joseph Krumenacker, and David Vanhoy, "X-29 High Angle-of-Attack Flight Test Procedures, Results, and Lessons Learned," SFTE 21st Annual Symposium, Garden Grove, CA, Aug. 1990.

REPORT DOCUMENTATION PAGE

Form Approved
OMB No. 0704-0188

1. AGENCY USE ONLY (Leave blank)	2. REPORT DATE	3. REPORT TYPE AND DATES COVERED
	June 1994	Technical Memorandum

4. TITLE AND SUBTITLE

X-29 Flight Control System: Lessons Learned

5. FUNDING NUMBERS

WU 505-64-30

6. AUTHOR(S)

Robert Clarke, John J. Burken, John T. Bosworth, and Jeffrey E. Bauer

7. PERFORMING ORGANIZATION NAME(S) AND ADDRESS(ES)

NASA Dryden Flight Research Center
P.O. Box 273
Edwards, California 93523-0273

8. PERFORMING ORGANIZATION REPORT NUMBER

H-1995

9. SPONSORING/MONOTORING AGENCY NAME(S) AND ADDRESS(ES)

National Aeronautics and Space Administration
Washington, DC 20546-0001

10. SPONSORING/MONITORING AGENCY REPORT NUMBER

NASA TM-4598

11. SUPPLEMENTARY NOTES

This was originally prepared for the AGARD Flight Mechanics Panel Symposium, Turin, Italy, May 9–12, 1994.

12a. DISTRIBUTION/AVAILABILITY STATEMENT

Unclassified—Unlimited
Subject Category 02

12b. DISTRIBUTION CODE

13. ABSTRACT (Maximum 200 words)

Two X-29A aircraft were flown at the NASA Dryden Flight Research Center over a period of eight years. The airplanes' unique features are the forward-swept wing, variable incidence close-coupled canard and highly relaxed longitudinal static stability (up to 35-percent negative static margin at subsonic conditions). This paper describes the primary flight control system and significant modifications made to this system, flight test techniques used during envelope expansion, and results for the low- and high-angle-of-attack programs. Throughout the paper, lessons learned will be discussed to illustrate the problems associated with the implementation of complex flight control systems.

14. SUBJECT TERMS

Flight control system; Flight-estimated stability margins; Static instability; X-29A airplane

15. NUMBER OF PAGES

19

16. PRICE CODE

AO3

17. SECURITY CLASSIFICATION OF REPORT	18. SECURITY CLASSIFICATION OF THIS PAGE	19. SECURITY CLASSIFICATION OF ABSTRACT	20. LIMITATION OF ABSTRACT
Unclassified	Unclassified	Unclassified	Unlimited